

## **Archaeal Populations in Hypersaline Sediments Underlying Orange Microbial Mats in the Napoli Mud Volcano**

Cassandra Sara Lazar, Stéphane L'Haridon, Patricia Pignet, and Laurent Toffin\*

Laboratoire de Microbiologie des Environnements Extrêmes, UMR 6197, Ifremer Centre de Brest, Département Etudes des Environnements Profonds, Université de Bretagne Occidentale, BP70, 29280 Plouzané, France

\*: Corresponding author : Laurent Toffin, Tel.: 33(0)2 98 22 43 96, Fax: 33(0) 98 22 47 57, email address : [laurent.toffin@ifremer.fr](mailto:laurent.toffin@ifremer.fr)

### **Abstract:**

Microbial mats in marine cold seeps are known to be associated with ascending sulfide- and methane-rich fluids. Hence, they could be visible indicators of anaerobic oxidation of methane (AOM) and methane cycling processes in underlying sediments. The Napoli mud volcano is situated in the Olimpi Area that lies on saline deposits; from there, brine fluids migrate upward to the seafloor. Sediments associated with a brine pool and microbial orange mats of the Napoli mud volcano were recovered during the Medeco cruise. Based on analysis of RNA-derived sequences, the "active" archaeal community was composed of many uncultured lineages, such as rice cluster V or marine benthic group D. Function methyl coenzyme M reductase (*mcrA*) genes were affiliated with the anaerobic methanotrophic *Archaea* (ANME) of the ANME-1, ANME-2a, and ANME-2c groups, suggesting that AOM occurred in these sediment layers. Enrichment cultures showed the presence of viable marine methylotrophic *Methanococoides* in shallow sediment layers. Thus, the archaeal community diversity seems to show that active methane cycling took place in the hypersaline microbial mat-associated sediments of the Napoli mud volcano.

## **1. Introduction**

Over 200 mud volcanoes have been found along the northern flank of the Mediterranean Ridge in the Eastern Mediterranean Sea (13). The formation of the Mediterranean Ridge is linked to the collisional tectonics between the African and Eurasian plates, resulting in intensive faulting (19). Within the Mediterranean Ridge, the Olimpi area, situated south of Crete, is a dynamic environment containing active seepage of mud, fluid, and brines. During the Messinian salinity crisis, evaporites

44 were deposited in the Mediterranean Basins (70), resulting in continuous evaporite  
45 dissolution and brines migrating upwards in the Olimpi area (14). Mud volcanism is  
46 often associated with brine seeps in this area (70). The Napoli mud volcano is a  
47 submarine circular dome situated in the Olimpi area (Fig. 1). Subsurface brines  
48 reaching the seafloor of the mud volcano create brine pools and lakes with diameters  
49 ranging from centimeters to meters (13). The highest fluid flows are located near the  
50 physical center of the mud volcano where mud mixed with brine enriched in biogenic  
51 methane are mostly expelled (13).

52 Most of the methane rising up does not reach the seafloor because it is mainly  
53 consumed by an efficient microbially mediated process known as anaerobic  
54 oxidation of methane (AOM) (37). AOM has been documented in various anoxic  
55 marine sediments, such as sediments of mud volcanoes (45), hydrothermal vents  
56 (62), and hypersaline environments (36). AOM is driven by ANaerobic  
57 MEthanotrophs (ANME) of the *Archaea*, and is mainly coupled to sulfate reduction  
58 driven by Sulfate Reducing Bacteria (SRB). ANME are divided into three  
59 phylogenetic groups, ANME-1, ANME-2 and ANME-3. The ANME-1 *Archaea* are  
60 distantly affiliated with the methanogenic orders *Methanosarcinales* and  
61 *Methanomicrobiales*, the ANME-2 with the methanogenic order *Methanosarcinales*,  
62 and the ANME-3 with the methanogenic genera *Methanococoides/Methanlobus*.  
63 Alternative electron acceptors such as  $\text{NO}_2^-$  (55),  $\text{Fe}^{3+}$ , and  $\text{Mn}^{4+}$  (5) have been  
64 recently reported to be coupled to AOM with higher energy yields, based on  
65 thermodynamic estimations. So far, no pure culture or defined consortium of ANME  
66 has been isolated, and the biochemical pathways of AOM remain unknown. In the  
67 current reverse methanogenesis hypothesis, *i.e.*  $\text{CO}_2$  reduction to  $\text{CH}_4$ , methane  
68 oxidation is catalyzed by a modified methyl coenzyme M reductase (MCR) (22, 23,

69 32), which in methanogens catalyzes the final step of methanogenesis (63). The  
70 *mcrA* gene, encoding the MCR, is unique and found in all methanogens and  
71 anaerobic methanotrophic *Archaea* (63). Phylogenetic *mcrA* based trees mirror the  
72 phylogeny of the 16S rRNA genes for all known methanogens (20, 38). And, the  
73 *mcrA* genes are conserved making them specific and useful functional gene markers,  
74 targeting methanogens and methanotrophs in the environment.

75 Dense filamentous microbial mats on the seafloor of cold seep sediments are visible  
76 to the naked eye. These mats are mainly composed of multicellular filaments  
77 (diameter of 12 to 160  $\mu\text{m}$  (41)), pigmented (*e.g.* orange or white) and unpigmented.  
78 Microbial communities in sediments underlying microbial mats have been shown to  
79 support high rates of sulfate-reduction (8, 27), sulfur-oxidation (50), nitrate-reduction  
80 (8, 27) and anaerobic methane oxidation (8, 27). Members of these communities  
81 have been previously identified as filamentous sulfur-oxidizing bacteria of the  
82 *Beggiatoa*, *Thioplaca*, *Leucothrix*, *Thiotrix* and *Desmanthos* genera (24), as well as  
83 diverse *Proteobacteria* (24, 43) and *Archaea* (42, 43). Interestingly, the archaeal  
84 communities in sediments underlying seep-associated microbial mats are dominated  
85 by methanogens and methane oxidizers (35). Thus, sediments underlying mats  
86 provide alternative niches for diverse active archaeal communities adapted to  
87 dynamic changes of fluid flow regimes.

88 This study analyzes archaeal community structure and diversity with depth, in  
89 hypersaline sediments associated with orange-pigmented mats of the Napoli mud  
90 volcano. The main objectives were to characterize the archaeal communities in  
91 hypersaline sediments underlying dense microbial mats. Vertical distribution patterns  
92 of archaeal communities were assessed using PCR-DGGE. Total RNA was extracted  
93 from 0 to 4 cm below seafloor (cmbsf) and 6 to 10 cmbsf sediment layers and

94 subjected to reverse-transcription PCR with primers specific of the archaeal 16S  
95 rRNA genes. Then, archaeal methanotroph and methanogen diversity was  
96 determined based on *mcrA* genes from two different sediment depths (2 to 4 and 8 to  
97 10 cmbsf). Finally, as methane was previously shown to mainly have a biogenic  
98 origin in the Napoli mud volcano, enrichment cultures for methanogens were carried  
99 out at all depths.

100

## 101 **MATERIALS AND METHODS**

### 102 **Sediment sampling and porewater analysis.**

103 Sediment samples were collected in the Napoli Mud Volcano, in the Eastern  
104 Mediterranean Sea during the Ifremer Medeco cruise with the research vessel  
105 *Pourquoi Pas?* in October/November 2007. Sediment pushcore CT-21 (Fig. 1) was  
106 recovered during dive PL 331-10 by the remotely operated vehicle (ROV) VICTOR  
107 6000 (Ifremer) from 1938 metres of water depth (N 33°43.4397, E 24°41.0385). In  
108 the sampled area, sediments were recovered with dense orange microbial mats.  
109 Brine pools and rivers were observed in close proximity to the microbial orange mats.  
110 The sediment push-core sample contained bacterial orange filaments that penetrated  
111 the first 2-3 cm layers. Immediately after retrieval, the sediment core (10 cm long)  
112 was sectioned aseptically in 2 cm thick layers in the cooling room (4°C), and frozen  
113 at -80°C for nucleic acid extractions.

114 Depth profiles of dissolved porewater sulfate and chloride were quantified from  
115 diluted pore waters. Porewater was obtained by centrifuging approximately 10g of  
116 crude sediment, 15 minutes, 3000 x g at 4°C. The porewater was then stored at -20°.  
117 Depth profiles of dissolved porewater sulfate and chloride were quantified from  
118 diluted pore waters. Sulfate and chloride concentrations were measured using ion

119 exchange chromatography, with a isocratic DX120 ion chromatography system  
120 (DIONEX Corporation, Sunnyvale, CA) fitted with Ionpac AS9-SC columns and a  
121 suppressor (ASRS-ultra II) unit in combination with a DS4-1 heated conductivity cell.  
122 Components were separated using a sodium carbonate gradient, with a flow of 1.5  
123 mL/min.

124

### 125 **Culture media for enrichment of methanogens.**

126 One volume of sediment subsample (10 cm<sup>3</sup>) was transferred into an anaerobic  
127 cabinet and then into 50 mL vials containing one volume (10 mL) of sterile and  
128 reduced Artificial Sea Water (ASW) medium. ASW corresponded to medium 141 of  
129 DSMZ devoid of organic carbon substrates. Enrichments were performed  
130 anaerobically in 50 mL vials according to Balch and Wolfe (3). Medium 141 from the  
131 DSMZ was used with slight modifications: organic substrates were omitted except  
132 yeast extract with a concentration adjusted to 0.2 g/L. The medium was prepared and  
133 sterilized under 80% N<sub>2</sub> and 20% CO<sub>2</sub> gas atmosphere. In order to enrich CO<sub>2</sub>-  
134 reducing, acetoclastic and methylotrophic methanogens, three enrichment media  
135 supplemented with H<sub>2</sub> (200 kPa), acetate (10 mM), and trimethylamine (TMA, 20  
136 mM) were used. One g of sediment from the different sections of CT21 was  
137 inoculated into 9 mL of medium (pH 7), the suspension was mixed and serially  
138 diluted until 10<sup>-3</sup>. The cultures were incubated at 15°C to mimic *in situ* conditions.  
139 Cultures were periodically checked for methane production for one year. Methane  
140 was detected directly in the headspace of vial cultures by a micro MTI M200 Gas  
141 Chromatograph equipped with MS-5A capillary column and Poraplot U capillary  
142 column. Positive enrichment dilutions of methanogens were monitored by PCR-

143 DGGE. For dilutions showing one DGGE band on the fingerprint, 16S rRNA genes  
144 were amplified cloned and sequenced using the A8F and A1492R primers.

145

#### 146 **Nucleic acids extraction and purification.**

147 Total genomic DNA was directly extracted and purified from 5g of wet sediment for all  
148 sections in duplicates, using the Zhou *et al.* (69) method with modifications. Sediment  
149 samples were mixed with DNA extraction buffer as described (69), followed by 3  
150 cycles of freezing in liquid N<sub>2</sub> and thawing at a 65°C. The pellet of crude nucleic acids  
151 obtained after centrifugation, was washed with cold 80% ethanol, and resuspended  
152 in sterile deionized water, to give a final volume of 100 µL. Crude DNA extracts were  
153 then purified using the Wizard DNA clean-up kit (Promega, Madison, WI). DNA  
154 extracts were aliquoted and stored at -20°C until required for PCR amplification.

155 Total RNA was directly extracted and purified from 2g of wet sediment from pooled  
156 sediment sections 0 to 4 and 6 to 10 cmbsf, using the RNA PowerSoil Total RNA  
157 Isolation Kit (MO BIO Labs. Inc., Carlsbad, CA) according to manufacturer  
158 recommendations. Aliquots of RNA extracts were treated by Turbo DNase (Applied  
159 Biosystems, Foster City, CA) and purified using the RNeasy Mini Kit (QIAGEN,  
160 Hilden, Germany) according to the manufacturer's protocol. The quality of RNA  
161 samples was examined by agarose-gel electrophoresis and concentrations were  
162 determined using spectrophotometry (Nanodrop ND-100, NanoDrop Technologies  
163 Wilmington, DE, USA).

164

#### 165 **Archaeal 16S rRNA PCR-DGGE amplification.**

166 Archaeal 16S rRNA genes were amplified by PCR from purified DNA extracts using  
167 the primers pair 8F (5'-CGGTTGATCCTGCCGGA-3') and 1492R (5'-

168 GGCTACCTTGTTACGACTT-3') (10). All PCR reactions (total volume reaction 25  
169  $\mu$ L) contained 1  $\mu$ L purified DNA template, 1X PCR buffer (Promega, Madison, WI), 2  
170 mM MgCl<sub>2</sub>, 0.2 mM of each dNTP, 0.4 mM of each primer (Eurogentec) and 0.6 U  
171 *GoTaq* DNA polymerase (Promega, Madison, WI). Amplification was carried out  
172 using the GeneAmp PCR 9700 System (Applied Biosystems, Foster City, CA). The  
173 PCR conditions were as follows: denaturation at 94 °C for 1 min, annealing at 49 °C  
174 for 1 min 30 s, and extension at 72 °C for 2 min for 30 cycles. All the archaeal 16S  
175 rRNA gene PCR products were then re-amplified in a nested PCR with primers 340F  
176 (5'-CCCTACGGGGYGCASCAG-3') (65) containing a GC clamp (5'-  
177 CGCCCGCCGCGCCCCGCGCCCGTCCCGCCGCCCCCGCCCG-3') at the 5' end,  
178 and primer 519R (5'-TTACCGCGGCKGCTG-3') (51). The PCR conditions were as  
179 follows: denaturation at 94 °C for 30 s, annealing at 72 °C to 62 °C (touchdown -0,5 °C  
180 per cycle) for 30 s, and extension at 72 °C for 1 min, for 20 cycles, then denaturation  
181 at 94 °C for 30 s, annealing at 62 °C for 30 s, and extension at 72 °C for 1 min, for 10  
182 cycles, and a final extension at 72 °C for 30 min (25).

183 To restrict contamination to a minimum, PCR experiments was carried out under  
184 aseptic conditions (Captair® bio, Erlab, Fisher Bioblock Scientific) using autoclaved  
185 and UV-treated plasticware and pipettes, and only sterile nuclease-free molecular  
186 grade water (MP Biomedicals, Solon, OH, USA). Positive (DNA extracted from pure  
187 cultures) and negative (molecular grade water) controls were used in all PCR  
188 amplifications.

189

### 190 **Denaturing Gradient Gel Electrophoresis fingerprinting analysis.**

191 DGGE was carried out as described by Toffin *et al.* (64) with some modifications.

192 PCR products were separated by DGGE using the D-Gene™ System (Bio-Rad

193 Laboratories, Hercules, CA) on 8% (w/v) polyacrylamide gels (40% acrylamide/bis  
194 solution 37.5:1 Bio-Rad) with a gradient of denaturant between 20% and 60%. A  
195 denaturing gradient gel consists of [100% denaturant equals 7M urea and 40% (v/v)  
196 formamide]. Gels were poured with the aid of a 30 mL volume Gradient Mixer (Hoefer  
197 SG30, GE Healthcare, Buckinghamshire, UK) and prepared with 1 X TAE buffer (MP  
198 Biomedicals, Solon, OH, USA). Electrophoresis was carried out at 60°C, 200 V for 5  
199 hours (with an initial electrophoresis for 10 min at 80 V) in 1 X TAE buffer.  
200 Polyacrylamide gels were stained with SYBRGold nucleic acid gel stain (Invitrogen,  
201 San Diego, CA) for 30 min, and viewed using the Typhoon 9400 Variable Mode  
202 Imager (GE Healthcare, Buckinghamshire, UK).

203

#### 204 **Construction of RNA-derived 16S rRNA gene libraries.**

205 RNA-derived cDNA was synthesised by reverse transcription using the 16S rRNA  
206 archaeal primer 915R (5'-GTGCTCCCCCGCCAATTCCT-3') (9) and the Moloney  
207 Murine Leukaemia Virus reverse transcriptase (M-MuLV, MP Biomedicals, Irvine, CA)  
208 according to the manufacturer's protocol. Purified RNA (100-150 ng) was initially  
209 denatured at 65°C for 10 min, and 7.7 µM primer 915R was added to the denatured  
210 RNA. The mixture was incubated at 70°C for 10 min. The reverse transcription  
211 reaction mixture (total volume of 22 µL) consisted of denatured RNA, 1X M-MuLV  
212 buffer, 200 µM of deoxynucleoside triphosphate mix, and 10 mM DTT (dithiothreitol).  
213 The reverse transcription reaction mix was incubated at 42°C for 2 min. A 200-unit  
214 aliquot of M-MuLV reverse transcriptase was added prior to a 80 min incubation at  
215 42°C for the reverse transcription of the RNA into complementary DNA (cDNA). The  
216 reaction was then stopped by heating at 70°C for 15 minutes. The cDNA end product  
217 was used as a template for archaeal 16S rRNA gene based PCR using the primer



218 set 340F/915R. The PCR amplification involved 20 cycles of 94 °C for 1 min, 71 °C to  
219 61 °C (touchdown -1 °C per cycle) for 1 min, and 72 °C for 2 min. PCR products were  
220 purified with the QIAquick Gel Extraction kit (QIAGEN, Hilden, Germany) and  
221 analyzed on 1% (w/v) agarose gels in 1 X TAE buffer and stained with ethidium  
222 bromide and UV-illuminated. Purified PCR products were cloned into TOPO<sup>®</sup> XL  
223 PCR Cloning Kit, and transformed into *Escherichia coli* TOP10 One Shot<sup>®</sup> cells  
224 (Invitrogen, San Diego, CA) according to the manufacturer's recommendations.  
225 Control PCR using the purified RNA and the same primers were performed to  
226 monitor possible DNA contamination of the RNA templates. No contaminating DNA  
227 was detected in any of these reactions.

228

#### 229 **Construction of *mcrA* environmental gene libraries.**

230 The *mcrA* genes were amplified using the ME1 (5'-GCMATGCARATHGGWATGTC-  
231 3') and ME2 (5'-TCATKGCRTAGTTDGGRTAGT-3') primers (20). The PCR  
232 conditions were as follows: denaturation at 94 °C for 40 s, annealing at 50 °C for 1'30  
233 min, and extension at 72 °C for 3 min, for 30 cycles. PCR products were purified on a  
234 1% agarose gel using the QIAquick Gel Extraction kit (QIAGEN, Hilden, Germany)  
235 and cloned using the TOPO XL PCR Cloning Kit (Invitrogen, San Diego, CA)  
236 according to the manufacturer's protocols.

237

#### 238 **Phylogenetic analysis of DNA.**

239 The gene sequencing was performed by *Taq* cycle sequencing and determined on a  
240 ABI PRISM 3100-Genetic Analyzer (Applied Biosystems, Foster City, CA) using the  
241 M13R (5'-CAGGAAACAGCTATGAC-3') universal primer. RNA-derived cDNA, DNA-  
242 derived *mcrA* and enrichment culture-derived 16S rRNA gene sequences were

243 analyzed using the NCBI BLASTN search program within GeneBank  
244 (<http://blast.ncbi.nlm.nih.gov/Blast>) (2). Potential chimeric sequences in the clone  
245 libraries were identified with the CHIMERA CHECK program of the Ribosomal  
246 Database Project II (Center for Microbial Ecology, Michigan State University,  
247 <http://wdc.mnig.ac.jp/RDP/html/analyses.html>). Potential chimeras were eliminated  
248 before phylogenetic trees were constructed. The RNA-derived 16S rRNA sequences  
249 and the enrichment culture-derived 16S rRNA gene sequences were then edited in  
250 the BioEdit v7.0.5 program (21) and aligned using the SINA webaligner  
251 (<http://www.arb-silva.de/>, (53)). The *mcrA* sequences were translated into amino acid  
252 sequences using BioEdit and aligned using ClustalX (33). Sequence data were  
253 analysed with the MEGA4.0.2 program (61). The phylogenetic trees were calculated  
254 using the neighbour-joining method. The robustness of the inferred topology was  
255 tested by bootstrap resampling (1000x). Rarefaction curves were calculated for the  
256 RNA-derived 16S rRNA, and *mcrA* gene libraries using the RarFac program  
257 (<http://www.icbm.de/pmbio/>), and a 97% similarity cutoff value for sequence-based  
258 OTUs. Gene library coverage was calculated using the following formula:  $C = [1 -$   
259  $(n_1/N)] * 100$ , where  $n_1$  is the number of unique OTUs, and N is number of clones in  
260 the library (58).

261

### 262 **Statistical analyses of DGGE banding patterns.**

263 The DGGE profile was analyzed as described by Fry *et al.* (15), using a  
264 presence/absence scoring of the DGGE bands. After making a grid to determine  
265 whether bands were present (score=1) or absent (score=0) for each lane on a same  
266 line of the DGGE profile, a presence/absence matrix was obtained. This matrix was  
267 then used to build a similarity matrix based on the Jaccard coefficient, using the

268 vegan package within the R software (54). Finally, a dendrogram was obtained using  
269 the ward agglomeration method within the hierarchical clustering package of the R  
270 software.

271

## 272 **Nucleotide sequence accession numbers.**

273 The sequence data reported here will appear in GenBank nucleotide sequence  
274 databases under the accession No. HM004785 to HM004825, and HQ443429 to  
275 HQ443514 for RNA-derived 16S rRNA gene sequences, HM004828 to HM004903  
276 and HQ454430 to HQ454493 for *mcrA* gene sequences, and HM004826 to  
277 HM004827 for enrichment culture-derived 16S rRNA gene sequences.

278

## 279 **RESULTS and DISCUSSION**

### 280 **Geochemical and biological characteristics.**

281 Observation of large orange-pigmented mats on the surface of the sampled sediment  
282 core and direct microscopic examination of filamentous morphology indicated that the  
283 *bacteria* were possibly members of genera *Beggiatoa* or *Thioploca*, as reported  
284 elsewhere (46, 56).

285 Profiles of sulfate and chloride concentrations in porewater sediments underlying the  
286 orange microbial mats were anticorrelated. The chloride porewater profile showed an  
287 increase in concentration with depth (Fig. 2), reaching 1200 mM at 10 cmbsf, which  
288 is more than 2 times higher than normal seawater concentrations (600 mM, (13)).

289 The sodium concentrations showed a similar increase with depth (Supplementary  
290 material. SM1), reaching 1224 mM at 10 cmbsf, which is also more than 2 times  
291 higher than normal seawater concentrations (492 mM, (13)). Furthermore, Charlou *et*  
292 *al.* characterized the brines in Napoli as being enriched in Cl and Na. Hence,

293 increases in chloride and sodium were presumably linked with the upflowing brines  
294 from deep sources in the Napoli mud volcano. The surface sediment layers colonized  
295 by the orange-pigmented mat bacteria showed chloride concentrations of 700 mM,  
296 and could be influenced by the brine pools contiguous to the filamentous bacteria on  
297 the seafloor. Moreover, bacterial mats are a common feature found in habitats  
298 influenced by hypersaline brine fluid intrusions (43, 48).

299 The sulfate porewater concentrations showed a slight decrease with depth (Fig. 2),  
300 which could suggest sulfate reduction. Sediments associated with orange- and white-  
301 pigmented *Beggiatoa* mats have been shown to host high rates of sulfate reduction,  
302 probably a combination of increased substrate availability in the seep fluids, and of  
303 rapid sulfate recycling within the sulfur-oxidizing bacterial mat (43, 48). However, the  
304 Napoli sediments did not seem to have a clear sulfate reducing zone. Profiles of the  
305  $Mg^{2+}$  and  $Ca^{2+}$  porewater concentrations (*Supplementary material. SM1*) showed  
306 decrease with depth. Concentrations reached 34 and 3 mM for  $Mg^{2+}$  and  $Ca^{2+}$   
307 respectively at 10 cmbsf (whereas seawater concentrations are typically 56 and 11  
308 mM (13), suggesting authigenic carbonate precipitation in these sediment layers.  
309 Indeed, anaerobic oxidation of methane increases alkalinity in porewater fluids by  
310 producing  $HCO_3^-$ , that in turn reacts with and precipitates  $Mg^{2+}$  and  $Ca^{2+}$  cations (11,  
311 30).

312

### 313 **Vertical distribution of the archaeal communities.**

314 The DGGE fingerprints (Fig. 3A) generated from DNA samples extracted from  
315 sediment layers associated with orange-pigmented microbial mats of the Napoli mud  
316 volcano displayed a complex and diverse distribution of the archaeal communities.  
317 The resulting dendrogram (Fig. 3B) of the DGGE pattern highlighted clear changes in

318 populations with depth in two separate clusters. The first cluster grouped depths 0 to  
319 4 cmbsf, and the second the 4 to 10 cmbsf sediment layers, suggesting a change in  
320 archaeal populations at 4 cmbsf, with increasing depth and salinity. This shift could  
321 be linked to the presence of the bacterial filaments in these sediments. Indeed these  
322 filaments belonging to what is commonly called "Big Bacteria" could have locally  
323 modified the geochemical conditions in the surrounding sediments (56), therefore  
324 affecting the microbial community diversity in the upper 4 cm. Salt concentrations  
325 might also have affected the depth distribution of the microbial communities, as  
326 reported elsewhere (28).

327 According to the statistical analysis of the DGGE pattern indicating a shift in the  
328 archaeal community at 4 cmbsf, we constructed two RNA-derived 16S rRNA gene  
329 libraries for depths 0-4, and 6-10 cmbsf. A total of 55 archaeal RNA-derived 16S  
330 rRNA gene sequences were analysed for the 0-4 cmbsf section, and 72 for the 6-10  
331 cmbsf section. Rarefaction curves generated for the RNA-derived 16S rRNA genes  
332 indicated saturation (*Supplementary material. SM2*), while percent coverage was  
333 determined to be 40% and 72.2% for the 0-4 and 6-10 cmbsf sections respectively.  
334 Hence coverage analysis suggests that the full diversity of archaeal 16S rRNA  
335 sequences was not exhausted and that a greater diversity remains to be detected  
336 within these sediments. Simpson's diversity indices (57) were calculated for each  
337 section, and indicated a decrease in archaeal diversity with depth ( $D=0.9554$  for the  
338 0-4 cmbsf section, and 0.9109 for the 6-10 cmbsf section).

339 The phylogenetic trees of the RNA-derived 16S rRNA gene libraries showed high  
340 archaeal diversity and a majority of sequences most closely related to environmental  
341 clones from mud volcano sediments of the Mediterranean Sea (*i.e.* Milano, Kazan,  
342 Chefren), marine sediments and seafloor sediments (*i.e.* Peru margin). **Thirty-**

343 eight OTUs belonging to archaeal uncultured groups were detected in the 0-4 cmbsf  
344 sediment layer 16S gene library, belonging to two major groups (Fig. 4 and 5):  
345 Marine Benthic Group D (MBG-D, 40.5%) and Rice Cluster V (RC-V, 40.5%). The  
346 other minor groups that were detected also belong to uncultured archaeal lineages  
347 (Fig. 4 and 5), *i.e.* Deep-sea Hydrothermal Vent Euryarchaeotic group 4 (DHVE-4),  
348 Group VI, Terrestrial Miscellaneous Euryarchaeotal Group (TMEG), Marine Group II  
349 (MG-II), Miscellaneous Crenarchaeotic Group (MCG), Marine Benthic Group B  
350 (MBG-B). One clone (NapMat-0\_4-rtC09) was not related to any known group. The  
351 only sequence closely related to cultured prokaryotes (NapMat-0\_4-rtB11b) was  
352 related to the methanogenic order of the *Methanosarcinales* (*Supplementary*  
353 *material*. SM3). Thirty-one OTUs also belonging to archaeal uncultured groups were  
354 detected in the 6-10 cmbsf sediment layer 16S gene library, belonging to two major  
355 groups (Fig. 4 and 5): MBG-D (55%), and MCG (17.5%). Other minor groups related  
356 to uncultured archaeal groups were detected as well (Fig. 4 and 5), *i.e.* TMEG,  
357 Marine Benthic Group E (MBG-E), and MBG-B. Two clones were affiliated with the  
358 methanogenic order *Methanosarcinales*, one with the anaerobic methanotrophic  
359 group ANME-3, one with the Rice Cluster II, which are surmised to be involved in  
360 methane production (18), and finally one clone (NapMat-6\_10-rtH01) was affiliated  
361 with an extreme halophilic *Archaea* of the *Halobacteria* (47). Most of the sequences  
362 only detected in the 6-10 cmbsf section (*i.e.* MBG-B, MCG, and TMEG) were closely  
363 related with sequences retrieved from subsurface sediments of the Peru margin (7,  
364 60).  
365 Intriguingly, RC-V members were presumably active in the 0-4 cmbsf sediments  
366 underlying orange-pigmented mats. The RC-V were first discovered in an anoxic  
367 flooded rice paddy soil (18), detected in many freshwater sediments (12, 17, 67, 68),

368 and were recently shown to be active in tubeworm populated sediments of the  
369 Storegga Slide (34). The intralinear levels of rDNA similarity of the RC-V  
370 sequences were low highlighting that this group seems to be phylogenetically very  
371 diverse. This could suggest diverse metabolic activities and physiologies. RC-V were  
372 also previously observed in cold coastal waters of the Mackenzie River in  
373 northwestern Canada, rich in suspended particles (16). The authors suggested that  
374 RC-V were linked to detrital decomposition. The Napoli sediments in which the RC-V  
375 were detected had a high organic matter content (data not shown), which could  
376 support the hypothesis of an organotrophic metabolism. This study is the first to  
377 report occurrence of probable active members of the RC-V in hypersaline sediments.  
378 Also, sequences affiliated with the RC-V were not detected in the 6-10 cmbsf  
379 sediment layers where salinity reached 1300 mM, suggesting that members of the  
380 RC-V probably do not tolerate high salt concentrations.

381 Sequences affiliated with the archaeal uncultured MBG-D were detected in many  
382 saline or hypersaline environments (6, 26, 36, 48, 59). Jiang *et al.* proposed that  
383 salinity could play a role in controlling the distribution of marine benthic groups, such  
384 as the MBG-D (26). Furthermore, the MBG-D was the main archaeal group  
385 presumably "active" in both sections (0-4 and 6-10 cmbsf) where  $\text{Cl}^-$  and  $\text{Na}^+$   
386 porewater concentrations were high (834 and 792 mM respectively).

387

### 388 **Diversity and distribution of the ANME.**

389 In order to show if ANME and/or methanogen affiliated sequences in hypersaline  
390 sediments are phylogenetically distinct from sequences in non hypersaline  
391 conditions, *mcrA* gene libraries were constructed for representative sediment  
392 sections characterized by increasing  $\text{Cl}^-$  and  $\text{Na}^+$  porewater concentrations, *i.e.* 2-4

393 and 8-10 cmbsf. A total of 75 *mcrA* sequences were analysed for the 2-4 cmbsf  
394 sediment section, and 65 for the 8-10 cmbsf layers (Fig. 6). Rarefaction curves  
395 generated for the *mcrA* clones of the two libraries indicated saturation  
396 (*Supplementary material. SM2*); while percent coverages were determined to be  
397 81.3% and 87.7% for the 2-4 and 8-10 cmbsf gene libraries. Simpson's diversity  
398 indices (57) were calculated for each section, and indicated a decrease in the  
399 methanotrophic/methanogenic diversity with depth ( $D=0.7952$  for the 2-4 cmbsf  
400 section, and 0.7096 for the 8-10 cmbsf section).

401 Three dominant *mcrA* phylotypes were present (*Supplementary material. SM4*), i.e.  
402 *mcrA* group a/b (ANME-1 as defined by Hallam *et al.*, (22)), *mcrA* group c/d (ANME-  
403 2c) and *mcrA* group e (ANME-2a). The majority of the *mcrA* clones were related to  
404 the ANME-2a at 2-4 cmbsf (58.3%), followed by the ANME-1. The ANME-2c  
405 sequences represented only a small portion of the ANME in the gene library. At the  
406 8-10 cmbsf section, the ANME-1 became the dominant group (65.6%), followed by  
407 the ANME-2c, and the ANME-2a represented only a small proportion of the ANME in  
408 the gene library.

409 Sediments underlying bacterial mats seem to constitute hot spots for AOM (43), as a  
410 consequence of high methane flux in the upwardly moving subsurface fluids,  
411 combined with sulfate availability in the surficial sediments aided by the mats (35).  
412 ANME-2a *Archaea* have been found as the unique methanotrophic representative in  
413 sediments of the active center of the Napoli mud volcano (Lazar *et al.*, unpublished  
414 data), dominated marine sediments of Skagerrak (52), and in sediments covered with  
415 white-pigmented mats of the Gulf of Mexico (43). It has been suggested that ANME-2  
416 may be more active at low temperatures compared to ANME-1 (44). Temperature  
417 gradient measurements of the active center of the Napoli mud volcano showed little



418 increase of temperature with depth down to 160 cmbsf, with an average temperature  
419 of 14°C (Lazar et al., unpublished data). It has also been suggested that ANME-2  
420 dominate sediment layers with high sulfate concentrations whereas ANME-1 seem to  
421 be found in sediment layers with low sulfate concentrations (31). Therefore, the  
422 distribution of the ANME-2 in the Napoli mud volcano sediments could support these  
423 assessments (Fig. 7).

424 ANME-1 *Archaea* have been detected in various environments. In hypersaline  
425 sediments of the Gulf of Mexico, the community of ANME was found to be limited to  
426 the ANME-1b, which were probably active (36). The authors suggested that the  
427 ANME-1b preponderance could be explained by the high salinity of the site (chloride  
428 concentration was 2200 mM), and that ANME-1b could be a high salinity adapted  
429 subpopulation. The increase in ANME-1 sequences with depth and with chloride  
430 concentrations (at the 8-10 cmbsf section, chloride concentration was 1256 mM) in  
431 the Napoli sediments could support this assumption.

432

#### 433 **Culturable methanogenic diversity.**

434 Methane production was detected in media designed to enrich methylotrophic  
435 methanogens on trimethylamines (TMA) in the shallow sulfate-rich 0-2, and 2-4  
436 cmbsf sediment sections. Microscopic observations of positive enrichments from the  
437 medium designed to enrich hydrogenotrophs suggested that methanogens were  
438 cocci-shaped cells. Under UV light, autofluorescent cells were detected as free cells.  
439 Total genomic DNA was extracted from the TMA enriched medium inoculated with  
440 the 0-2 and 2-4 cmbsf sediment sections. Phylogenetic affiliation of clone NapMat-  
441 0\_2-enr30 showed showed 99% sequence similarity with clone  
442 Tommo05\_1274\_3\_Arch90 of the *Euryarchaeota* (FM179838) recovered from the

443 Tommeliten methane seep, in the North Sea (66), and 98% of sequence similarity  
444 with the closest cultured methanogen *Methanococoides methylutens* (M59127).  
445 Phylogenetic affiliation of clone NapMat-2\_4-enr31 showed 98 % sequence similarity  
446 with the cultured methanogen *Methanococoides burtonii* (CP000300).

447 These results are in agreement with previous studies detecting methylotrophic  
448 *Methanococoides*-type methanogens in saline or hypersaline habitats such as a  
449 brackish lake (4), marine sediments in Skan Bay (29), anaerobic sediments of  
450 mangroves (39, 40), brine seeps of the Gulf of Mexico (28), and recently sediments  
451 of the center of the Napoli mud volcano (Lazar *et al.*, unpublished data).  
452 Representative species of methylotrophic methanogens in culture collections take up  
453 methylated compounds as substrates that are not used by other competitive  
454 microorganisms such as sulfate-reducing bacteria. Methylated compounds could  
455 derive from organic detritus from the microbial mat (Fig. 7). And, known cultured  
456 methylotrophic methanogens, belonging to the *Methanohalophilus* and  
457 *Methanohalobium* genera, have been shown to efficiently tolerate high salinity  
458 environments (up to 25 % NaCl) (49).

459

460 Surprisingly, in this study, only one 16S rRNA gene sequence of a known halophilic  
461 *Archaea* of the *Halobacteria* was detected, despite the high measured chloride  
462 concentrations. The same observation was also reported for brines from the Gulf of  
463 Mexico (28). However, as most of the sequences detected (*i.e.* DHVE4, MBG-D,  
464 MCG, RC-V, ANME) belong to as yet uncultured archaeal lineages, we can assume  
465 that some of the Napoli sequences represent unknown halophilic or halotolerant  
466 microorganisms. Moreover, Simpson's diversity indices indicated a decrease in  
467 archaeal and methanotrophic/methanogenic diversity with depth hence with

468 increasing salinity. This could suggest that salt adapted *Archaea* dominated the  
469 deeper layers of the Napoli mud volcano.

470

#### 471 **Conclusion.**

472 In this study, culture-dependent and –independent techniques were employed in  
473 order to assess the distribution of the "active" RNA-derived 16S rRNA archaeal  
474 sequences in sediments associated with orange-pigmented mats of the brine  
475 impacted Napoli mud volcano. In the shallow sulfate-rich sediment layers of the  
476 Napoli mud volcano, the active fraction of the archaeal community was mainly  
477 represented by sequences belonging to as yet uncultured lineages similar to those  
478 present in cold seeps and deep seafloor sediments, but unexpectedly also rice  
479 paddies. *mcrA* gene libraries suggested that AOM might have occurred in the Napoli  
480 mud volcano sediments. Enrichment cultures indicated that viable methanogens  
481 were present in the shallow sulfate-rich sediment layers. Therefore, a complex  
482 archaeal community was observed in this hypersaline habitat, possibly intertwining  
483 sulfur and methane cycles.

484

#### 485 **Acknowledgements.**

486 We would like to thank Josée Sarrazin and Catherine Pierre, the chief scientists of  
487 the MEDECO cruise, the ROV team, the officers and crew of the RV *Pourquoi Pas?*  
488 as well as the shipboard scientific community for their help at sea. We would also like  
489 to thank Andreas Teske (University of North Carolina), and Christian Jeanthon  
490 (Station Biologique of Roscoff) for their helpful scientific comments. This work was  
491 funded by the HERMES project Contract No. GOCE-CT-2005-511234-1, and the  
492 ANR Deep Oases.

## 494 REFERENCES

- 496 1. **Aloisi, G., C. Pierre, J.-M. Rouchy, J.-P. Foucher, J. Woodside, and t. M.**  
497 **S. Party.** 2000. Methane-related authigenic carbonates of eastern  
498 Mediterranean Sea mud volcanoes and their possible relation to gas hydrate  
499 destabilisation. *Earth Planet. Sci. Lett.* **184**:321-338.
- 500 2. **Altschul, S. F., W. Gish, W. Miller, E. W. Myers, and D. J. Lipman.** 1990.  
501 Basic local alignment search tool. *J. Mol. Biol.* **215**:403-410.
- 502 3. **Balch, W. E., and R. S. Wolfe.** 1976. New approach to the cultivation of  
503 methanogenic bacteria: 2-mercaptoethanesulfonic acid (HS-CoM)-dependent  
504 growth of *Methanobacterium ruminatum* in a pressurized atmosphere. *Appl.*  
505 *Environ. Microbiol.* **32**:781-791.
- 506 4. **Banning, N., F. Brock, J. C. Fry, R. J. Parkes, E. R. C. Hornibrook, and W.**  
507 **A. J.** 2005. Investigation of the methanogen population structure and activity  
508 in a brackish lake sediment. *Environ. Microbiol.* **7**:947 - 960.
- 509 5. **Beal, E. J., C. H. House, and V. J. Orphan.** 2009. Manganese- and Iron-  
510 Dependent Marine Methane Oxidation. *Science* **325**:184-187.
- 511 6. **Benlloch, S., A. López-López, E. O. Casamayor, L. Øvreås, V. Goddard, F.**  
512 **L. Daae, G. Smerdon, R. Massana, I. Joint, F. Thingstad, C. Pedrós-Alió,**  
513 **and F. Rodríguez-Valera.** 2002. Prokaryotic genetic diversity throughout the  
514 salinity gradient of a coastal solar saltern. *Environ. Microbiol.* **4**:349-360.
- 515 7. **Biddle, J. f., J. S. Lipp, M. A. Lever, K. G. Llyod, K. B. Sorensen, R.**  
516 **Anderson, H. F. Fredricks, M. Elvert, and e. al.** 2006. Heterotrophic Archaea  
517 dominate sedimentary subsurface ecosystems off Peru. *Proceedings of the*  
518 *National Academy of Sciences of the United States of America* **103**:3846-  
519 3851.
- 520 8. **Boetius, A., K. Ravenschlag, C. J. Schubert, D. Rickert, F. Widdel, and A.**  
521 **Gieske.** 2000. A marine microbial consortium apparently mediating anaerobic  
522 oxidation of methane. *Nature* **407**:623-626.
- 523 9. **Casamayor, E. O., R. Massana, S. Benlloch, L. Ovreas, B. Diez, V. J.**  
524 **Goddard, J. M. Gasol, I. Joint, and e. al.** 2002. Changes in archaeal,  
525 bacterial and eukaryal assemblages along a salinity gradient by comparison of  
526 genetic fingerprinting methods in a multipond solar saltern. *Environ. Microbiol.*  
527 **4**:338-348.
- 528 10. **Casamayor, E. O., H. Schäfer, L. Baneras, C. P. Salio, and G. Muyzer.**  
529 2000. Identification of and Spatio-Temporal Differences between Microbial  
530 Assemblages from Two Neighboring Sulfurous Lakes: Comparison by  
531 Microscopy and Denaturing Gradient Gel Electrophoresis. *Appl. Environ.*  
532 *Microbiol.* **66**:499-508.
- 533 11. **Chaduteau, C.** 2008. Origin and circulation of fluids in sediments of margins,  
534 Contribution of Helium and methane to the comprehension of the processes,  
535 Study of two zones.
- 536 12. **Chan, O. C., P. Claus, P. Casper, A. Ulrich, T. Lueders, and R. Conrad.**  
537 2005. Vertical distribution of structure and function of the methanogenic  
538 archaeal community in Lake Dagow sediment. *Environ. Microbiol.* **7**:1139-  
539 1149.

- 540 13. **Charlou, J. L., J. P. Donval, T. Zitter, N. Roy, P. Jean-Baptiste, J. P.**  
541 **Foucher, J. Woodside, and M. S. Party.** 2003. Evidence of methane venting  
542 and geochemistry of brines on mud volcanoes of the eastern Mediterranean  
543 Sea. *Deep. Sea. Res. I* **50**:941-958.
- 544 14. **Dählmann, A., and G. J. de Lange.** 2003. Fluid-sediment interactions at  
545 Eastern Mediterranean mud volcanoes: a stable isotope study from ODP Leg  
546 160. *Earth Planet. Sci. Lett.* **212**:377-391.
- 547 15. **Fry, J. C., G. Webster, B. A. Cragg, A. J. Weightman, and R. J. Parkes.**  
548 2006. Analysis of DGGE profiles to explore the relationship between  
549 prokaryotic community composition and biogeochemical processes in deep  
550 subseafloor sediments from the Peru Margin. *FEMS Microbiol. Ecol.* **58**:86-98.
- 551 16. **Galand, P. E., C. Lovejoy, and W. F. Vincent.** 2006. Remarkably diverse and  
552 contrasting archaeal communities in a large arctic river and the coastal Arctic  
553 Ocean. *Aquat. Microb. Ecol.* **44**:115-126.
- 554 17. **Glissmann, K., K.-J. Chin, P. Casper, and R. Conrad.** 2004. Methanogenic  
555 Pathway and Archaeal Community Structure in the Sediment of Eutrophic  
556 Lake Dagow: Effect of Temperature. *Microb. Ecol.* **48**:389-399.
- 557 18. **Grosskopf, R., S. Stubner, and W. Liesack.** 1998. Novel Euryarchaeotal  
558 Lineages Detected on Rice Roots and in the Anoxic Bulk Soil of Flooded Rice  
559 Microcosms. *Appl. Environ. Microbiol.* **64**:4983-4989.
- 560 19. **Haese, R. R., C. Hensen, and G. J. de Lange.** 2006. Pore water  
561 geochemistry of eastern Mediterranean mud volcanoes: Implications for fluid  
562 transport and fluid origin. *Mar. Geol.* **225**:191- 208.
- 563 20. **Hales, B. A., E. C, D. A. Titchie, G. Hall, P. R. W, and S. J. R.** 1996. Isolation  
564 and identification of methanogen-specific DNA from blanket bog peat by PCR  
565 amplification and sequence analysis. *Appl. Environ. Microbiol.* **62**:668-675.
- 566 21. **Hall, T. A.** 1999. BioEdit: a user-friendly biological sequence alignment editor  
567 and analysis program for Windows 95/98/NT. *Nucleic Acids Symp. Ser.*  
568 **41**:95–98.
- 569 22. **Hallam, S. J., P. R. Girguis, C. M. Preston, P. M. Richardson, and E. F.**  
570 **DeLong.** 2003. Identification of methyl coenzyme M reductase A (mcrA)  
571 genes associated with methane-oxidizing Archaea. *Appl. Environ. Microbiol.*  
572 **69**:5483-5491.
- 573 23. **Hallam, S. J., N. Putnam, C. M. Preston, J. C. Detter, D. Rokhsar, P. M.**  
574 **Richardson, and E. F. DeLong.** 2004. Reverse methanogenesis: testing the  
575 hypothesis with environmental genomics. *Science* **305**:1457-1462.
- 576 24. **Heijs, S. K., J. S. Sinninghe Damsté, and L. J. Forney.** 2005.  
577 Characterization of a deep-sea microbial mat from an active cold seep at the  
578 Milano mud volcano in the Eastern Mediterranean Sea. *FEMS Microbiol. Ecol.*  
579 **54**:47-56.
- 580 25. **Janse, I., J. Bok, and G. Zwart.** 2004. A simple remedy against artifactual  
581 double bands in denaturing gradient gel electrophoresis. *J. Microbiol. Methods*  
582 **57**:279– 281.
- 583 26. **Jiang, H., H. Dong, B. Yu, Q. Ye, J. Shen, H. Rowe, and C. Zhang.** 2008.  
584 Dominance of putative marine benthic Archaea in Qinghai Lake, north-western  
585 China. *Environ. Microbiol.* **10**:2355–2367.
- 586 27. **Joye, S. B., A. Boetius, B. N. Orcutt, J. P. Montoya, H. N. Schulz, M. J.**  
587 **Erickson, and S. K. Lugo.** 2004. The anaerobic oxidation of methane and  
588 sulfate reduction in sediments from Gulf of Mexico cold seeps. *Chem. Geol.*  
589 **205**:219-238.

- 590 28. **Joye, S. B., V. A. Samarkin, B. N. Orcutt, I. R. MacDonald, K.-U. Hinrichs,**  
591 **M. Elvert, A. P. Teske, K. G. Lloyd, M. A. Lever, J. P. Montoya, and C. D.**  
592 **Meile.** 2009. Metabolic variability in seafloor brines revealed by carbon and  
593 sulphur dynamics. *Nat. Geosci.* **2**:349-354.
- 594 29. **Kendall, M. M., G. D. Wardlaw, C. F. Tang, A. S. Bonin, Y. Liu, and D. L.**  
595 **Valentine.** 2007. Diversity of Archaea in marine sediments from Skan Bay,  
596 Alaska, including cultivated methanogens, and description of *Methanogenium*  
597 *boonei* sp. nov. *Appl. Environ. Microbiol.* **73**:407-414.
- 598 30. **Knittel, K., and A. Boetius.** 2009. Anaerobic Oxidation of Methane: Progress  
599 with an Unknown Process. *Annual review of microbiology* **63**:311–334.
- 600 31. **Krüger, M., M. Blumenberg, S. Kasten, A. Wieland, L. Känel, J.-H. Klock,**  
601 **W. Michaelis, and R. Seifert.** 2008. A novel, multi-layered methanotrophic  
602 microbial mat system growing on the sediment of the Black Sea. *Environ.*  
603 *Microbiol.* **10**:1934-1947.
- 604 32. **Krüger, M., A. Meyerdierks, F. O. Glöckner, R. Amann, F. Widdel, M.**  
605 **Kube, R. Reinhardt, J. Kanht, R. Böcher, R. K. Thauer, and S. Shima.**  
606 2003. A conspicuous nickel protein in microbial mats that oxidize methane  
607 anaerobically. *Nature* **426**:878-881.
- 608 33. **Larkin, M. A., G. Blackshields, N. P. Brown, R. Chenna, P. A. McGettigan,**  
609 **H. McWilliam, F. Valentin, I. M. Wallace, A. Wilm, R. Lopez, J. D.**  
610 **Thompson, T. J. Gibson, and D. G. Higgins.** 2007. Clustal W and Clustal X  
611 version 2.0. *Bioinformatics* **23**:2947-2948.
- 612 34. **Lazar, C. S., J. Dinasquet, P. Pignet, D. Prieur, and L. Toffin.** 2010. Active  
613 Archaeal Communities at Cold Seep Sediments Populated by Siboglinidae  
614 Tubeworms from the Storegga Slide. *Microb. Ecol.* DOI **10.1007/s00248-010-**  
615 **9654-1.**
- 616 35. **Lloyd, K. G., D. B. Albert, J. F. Biddle, J. P. Chanton, O. Pizarro, and A.**  
617 **Teske.** 2010. Spatial Structure and Activity of Sedimentary Microbial  
618 Communities Underlying a *Beggiatoa* spp. Mat in a Gulf of Mexico  
619 Hydrocarbon Seep. *PloS One* **5.**
- 620 36. **Lloyd, K. G., L. Lapham, and A. Teske.** 2006. An anaerobic methane-  
621 oxidizing community of ANME-1b Archaea in hypersaline Gulf of Mexico  
622 sediments. *Appl. Environ. Microbiol.* **72**:7218-7230.
- 623 37. **Lösekan, T., K. Knittel, T. Nadalig, B. Fuchs, H. Niemann, A. Boetius,**  
624 **and R. Amann.** 2007. Diversity and abundance of aerobic and anaerobic  
625 methane oxidizers at the Haakon Mosby Mud Volcano, Barents Sea. *Appl.*  
626 *Environ. Microbiol.* **73**:3348-3362.
- 627 38. **Luton, P. E., J. M. Wayne, R. J. Sharp, and P. W. Riley.** 2002. The *mcrA*  
628 gene as an alternative to 16S rRNA in the phylogenetic analysis of  
629 methanogen populations in landfill. *Microbiology* **148**:3521-3530.
- 630 39. **Lyimo, T. J., A. Pol, M. S. M. Jetten, and H. J. M. Op den Camp.** 2009.  
631 Diversity of methanogenic archaea in a mangrove sediment and isolation of a  
632 new *Methanococcoides* strain. *FEMS Microbiol. Ecol.* **291**:247–253.
- 633 40. **Lyimo, T. J., A. Pol, H. J. M. Op den Camp, H. R. Harhangi, and G. D.**  
634 **Vogels.** 2000. *Methanosarcina semesiae* sp. nov., a dimethylsulfide-utilizing  
635 methanogen from mangrove sediment. *Int. J. Syst. Evol. Microbiol.* **50**:171–  
636 178.
- 637 41. **McHatton, S. C., J. P. Barry, H. W. Jannasch, and D. C. Nelson.** 1996. High  
638 nitrate concentrations in vacuolate, autotrophic marine *Beggiatoa* spp. *Appl.*  
639 *Environ. Microbiol.* **62**:954-958.

- 640 42. **Michaelis, W., R. Seifert, K. Nahaus, T. Treude, V. Thiel, M. Blumenberg,**  
641 **K. Knittel, A. Gieseke, K. Peterknecht, T. Pape, A. Boetius, and e. al.**  
642 2002. Microbial reefs in the Black Sea fueled by anaerobic oxidation of  
643 methane. *Science* **297**:1013-1015.
- 644 43. **Mills, H. J., R. J. Martinez, S. Story, and P. A. Sobecky.** 2004. Identification  
645 of members of the metabolically active microbial populations associated with  
646 *Beggiatoa* species mat communities from Gulf of Mexico cold-seep sediments.  
647 *Appl. Environ. Microbiol.* **70**:5447-5458.
- 648 44. **Nauhaus, K., T. Treude, A. Boetius, and M. Krüger.** 2005. Environmental  
649 regulation of the anaerobic oxidation of methane: a comparison of ANME-I  
650 and ANME-II communities. *Environ. Microbiol.* **7**:98-106.
- 651 45. **Niemann, H., J. Duarte, C. Hensen, E. Omoregie, V. H. Magalhaes, M.**  
652 **Elvert, L. M. Pinheiro, A. Kopf, and A. Boetius.** 2006. Microbial methane  
653 turnover at mud volcanoes of the Gulf of Cadiz. *Geochim. Cosmochim. Acta*  
654 **70**:5336-5355.
- 655 46. **Nikolaus, R., J. W. Ammerman, and I. R. MacDonald.** 2003. Distinct  
656 pigmentation and trophic modes in *Beggiatoa* from hydrocarbon seeps in the  
657 Gulf of Mexico. *Aquat. Microb. Ecol.* **32**:85–93.
- 658 47. **Oh, D., K. Porter, B. Russ, D. Burns, and M. Dyall-Smith.** 2010. Diversity of  
659 *Haloquadratum* and other haloarchaea in three, geographically distant,  
660 Australian saltern crystallizer ponds. *Extremophiles* **14**:161–169.
- 661 48. **Omoregie, E. O., V. Mastalerz, G. de Lange, K. L. Straub, A. Kappler, H.**  
662 **Røy, A. Stadnitskaia, J.-P. Foucher, and A. Boetius.** 2008. Biogeochemistry  
663 and Community Composition of Iron- and Sulfur-Precipitating Microbial Mats  
664 at the Chefren Mud Volcano (Nile Deep Sea Fan, Eastern Mediterranean).  
665 *Appl. Environ. Microbiol.* **74**:3198-3215.
- 666 49. **Oren, A.** 1999. Bioenergetic Aspects of Halophilism. *Microbiol. Mol. Biol. Rev.*  
667 **63**:334–348.
- 668 50. **Otte, S., J. G. Kuenen, L. P. Nielsen, H. W. Paerl, J. Zopfi, H. N. Schulz, A.**  
669 **Teske, B. Strotmann, V. A. Gallardo, and B. B. Jorgensen.** 1996. Nitrogen,  
670 Carbon, and Sulfur Metabolism in Natural Thioploca Samples. *Appl Environ*  
671 *Microbiol* **65**:3148–3157.
- 672 51. **Ovreas, L., L. Forney, F. L. Daae, and V. Torsvik.** 1997. Distribution of  
673 bacterioplankton in meromictic Lake Saelenvannet, as determined by  
674 denaturing gradient gel electrophoresis of PCR-amplified gene fragments  
675 coding for 16S rRNA. *Appl. Environ. Microbiol.* **63**:3367-3373.
- 676 52. **Parkes, R. J., B. A. Cragg, N. Banning, F. Brock, G. Webster, J. C. Fry, E.**  
677 **Hornibrook, and e. al.** 2007. Biogeochemistry and biodiversity of methane  
678 cycling in subsurface marine sediments (Skagerrak, Denmark). *Environ.*  
679 *Microbiol.* **9**:1146-1161.
- 680 53. **Pruesse, E., C. Quast, K. Knittel, B. M. Fuchs, W. Ludwig, J. Peplies, and**  
681 **F. O. Glöckner.** 2007. SILVA: a comprehensive online resource for quality  
682 checked and aligned ribosomal RNA sequence data compatible with ARB.  
683 *Nucleic Acids Res.* **35**:7188–7196.
- 684 54. **R Development Core, T.** 2008. R: A language and environment for statistical  
685 computing. R Foundation for Statistical Computing, Vienna, Austria. ISBN 3-  
686 900051-07-0, URL <http://www.R-project.org>.
- 687 55. **Raghoebarsing, A. A., A. Pol, K. T. van de Pas-Schoonen, A. J. P.**  
688 **Smolders, K. F. W. Ettwig, I. C. Rijpstra, S. Schouten, J. S. Sinninghe**  
689 **Damsté, H. J. M. Op den Camp, M. S. M. Jetten, and M. Strous.** 2006. A

- 690 microbial consortium couples anaerobic methane oxidation to denitrification.  
691 Nature **440**:918- 921.
- 692 56. **Schulz, H. N., and B. B. Jørgensen.** 2001. Big Bacteria. Annual review of  
693 microbiology **55**:105–137.
- 694 57. **Simpson, E. H.** 1949. Measurement of diversity. Nature **163**:688.
- 695 58. **Singleton, D. R., M. A. Furlong, S. L. Rathbun, and W. B. Whitman.** 2001.  
696 Quantitative Comparisons of 16S rRNA Gene Sequence Libraries from  
697 Environmental Samples. Appl. Environ. Microbiol. **67**:4374–4376.
- 698 59. **Sørensen, K. B., D. E. Canfield, A. P. Teske, and A. Oren.** 2005.  
699 Community Composition of a Hypersaline Endoevaporitic Microbial Mat. Appl.  
700 Environ. Microbiol. **70**:7352–7365.
- 701 60. **Sorensen, K. B., and A. Teske.** 2006. Stratified communities of active  
702 Archaea in deep marine subsurface sediments. Appl. Environ. Microbiol.  
703 **72**:4596-4603.
- 704 61. **Tamura, K., J. Dudley, M. Nei, and S. Kumar.** 2007. MEGA4: Molecular  
705 Evolutionary Genetics Analysis (MEGA) Software Version 4.0. Mol. Biol. Evol.  
706 **24**::1596–1599.
- 707 62. **Teske, A., K. U. Hinrichs, V. Edgcomb, A. D. Gomez, D. Kysela, S. P.**  
708 **Sylva, and e. al.** 2002. Microbial diversity of hydrothermal sediments in the  
709 Guaymas Basin: evidence for anaerobic methanotrophic communities. Appl.  
710 Environ. Microbiol. **68**:1994-2007.
- 711 63. **Thauer, R. K.** 1998. Biochemistry of methanogenesis: a tribute to Marjory  
712 Stephenson. Microbiology **144**:2377-2406.
- 713 64. **Toffin, L., G. Webster, A. J. Weightman, J. C. Fry, and D. Prieur.** 2004.  
714 Molecular monitoring of culturable bacteria from deep-sea sediment of the  
715 Nankai Trough, Leg 190 Ocean Drilling Program. FEMS Microbiol. Ecol.  
716 **48**:357–367.
- 717 65. **Vetriani, C., H. W. Jannasch, M. B. J, D. A. Stahl, and A.-L. Reysenbach.**  
718 1999. Population structure and phylogenetic characterization of marine bentic  
719 Archaea in deep-sea sediments. Appl. Environ. Microbiol. **65**:4375-4384.
- 720 66. **Wegener, G., M. Shovitri, K. Knittel, H. Niemann, M. Hovland, and A.**  
721 **Boetius.** 2008. Biogeochemical processes and microbial diversity of the  
722 Gullfaks and Tommeliten methane seeps (Northern North Sea).  
723 Biogeosciences **5**:1127-1144.
- 724 67. **Wu, L., K. Ma, Q. Li, X. Ke, and Y. Lu.** 2009. Composition of Archaeal  
725 Community in a Paddy Field as Affected by Rice Cultivar and N Fertilizer.  
726 Microb. Ecol. **58**:819–826.
- 727 68. **Zepp Falz, K., C. Holliger, R. Grosskopf, W. Liesack, A. N. Nozhevnikova,**  
728 **B. Müller, B. Wehrli, and D. Hahn.** 1999. Vertical Distribution of  
729 Methanogens in the Anoxic Sediment of Rotsee (Switzerland). Appl. Environ.  
730 Microbiol. **65**:2402–2408.
- 731 69. **Zhou, J., M. A. Bruns, and J. M. Tiedje.** 1996. DNA recovery from soils of  
732 diverse composition. Appl. Environ. Microbiol. **62**:316-322.
- 733 70. **Zitter, T. A. C., C. Huguen, and J. M. Woodside.** 2005. Geology of mud  
734 volcanoes in the eastern Mediterranean from combined sidescan sonar and  
735 submersible surveys. Deep. Sea. Res. I **52**:457-475.
- 736  
737



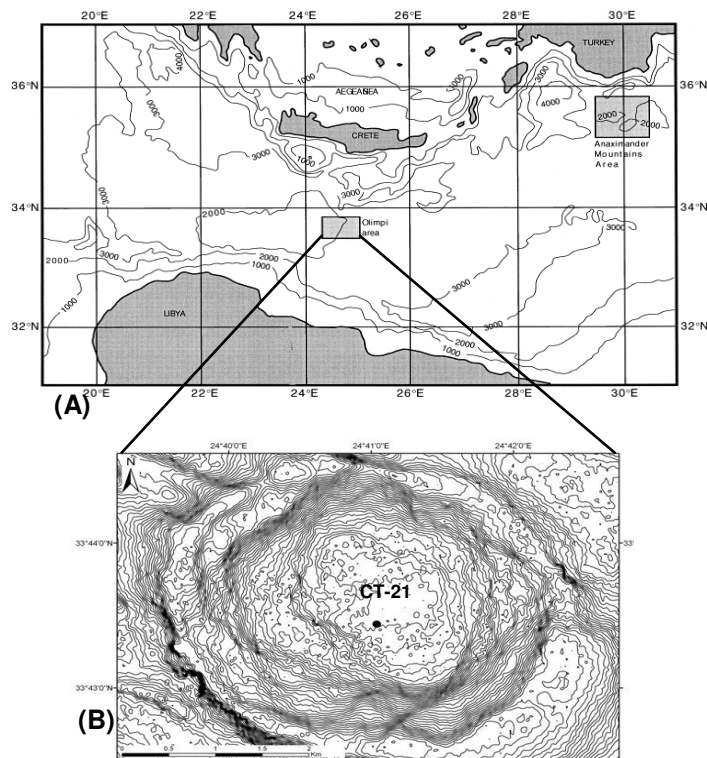


**Figure 1.** A) Location map showing the Olimpi area in the Eastern Mediterranean Sea. From Aloisi et al. (1). B) Closer view on the Napoli mud volcano and the position of the sampled push core (Bénédicte Ritt, pers. comm.).

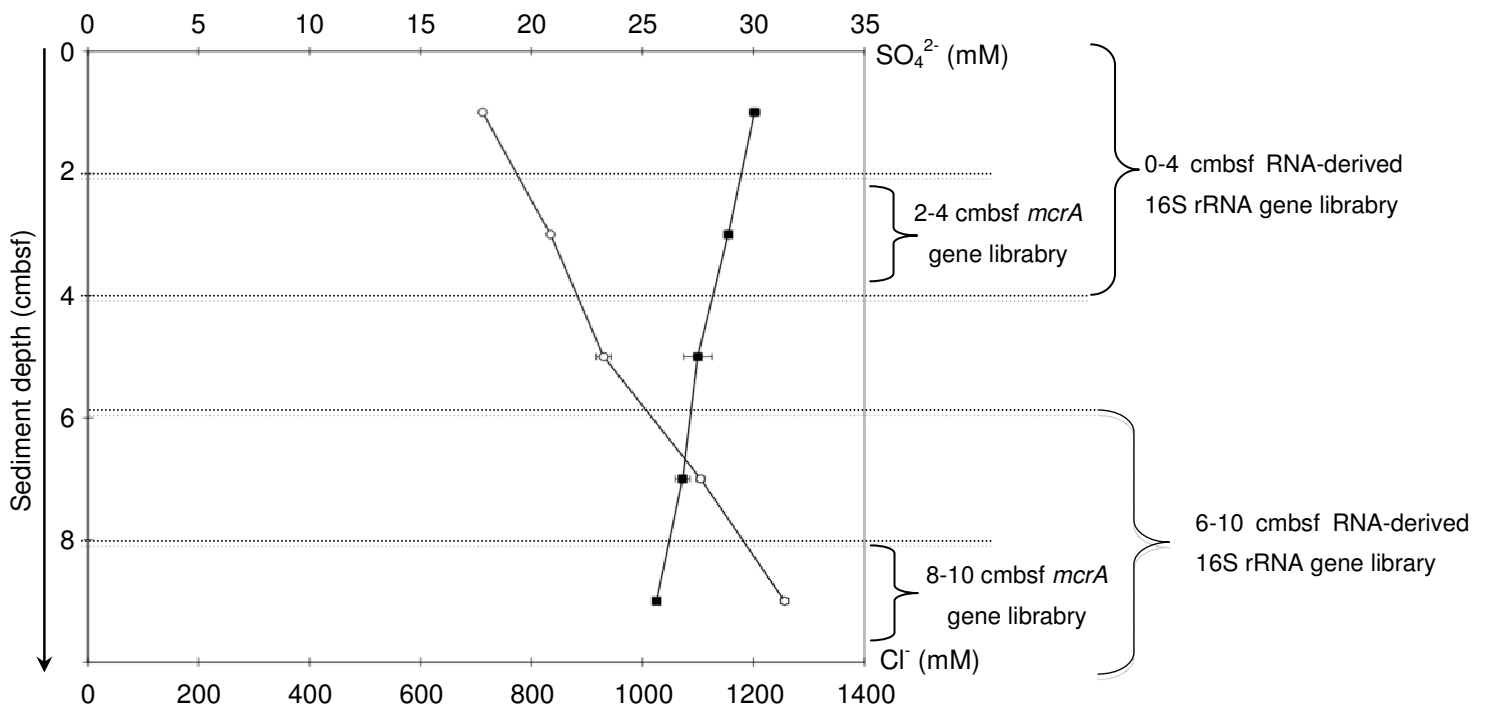


**Figure 2.** Sulfate (filled squares) and chloride (open circles) porewater concentrations (mean  $\pm$  standard deviation) in mM with depth for core CT-21 of the Napoli mud volcano sediments in cmbsf. The scale represents sediment depth below the seafloor. Sediment sections dedicated to *mcrA* and RNA derived 16S rRNA are indicated on the right.

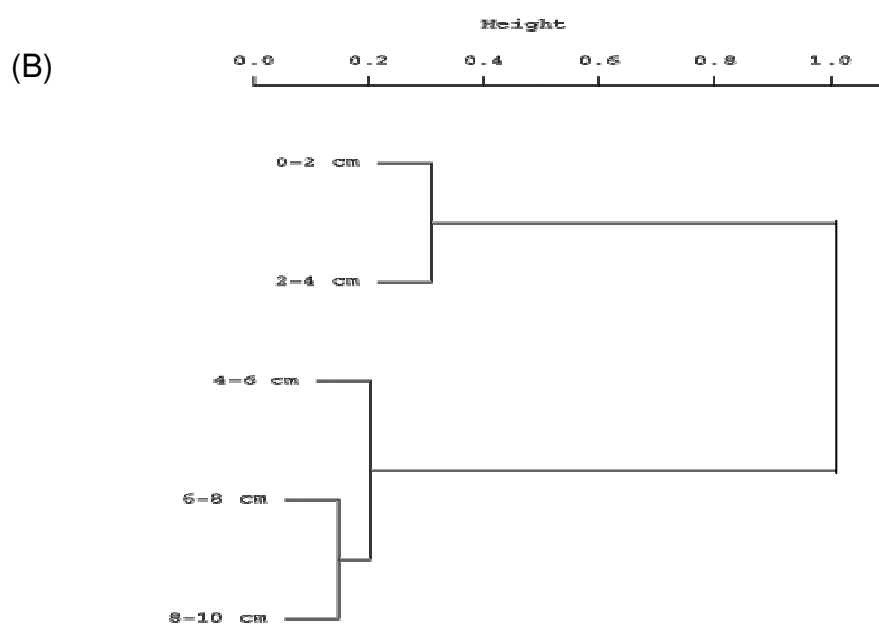
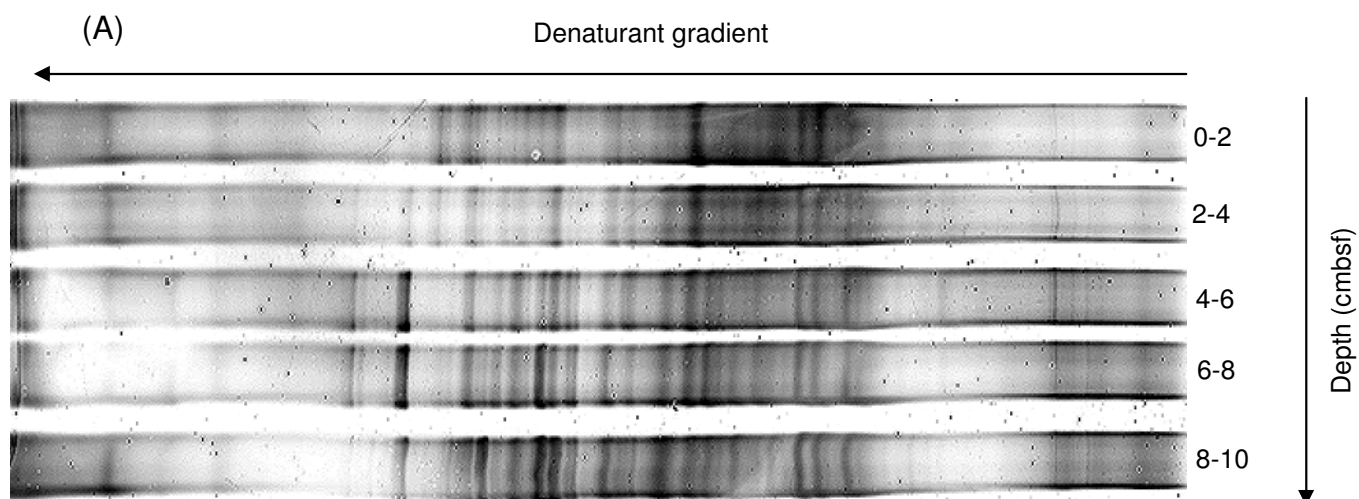


**Figure 3.** A) DGGE analysis of archaeal 16S rRNA genes obtained by nested PCR in the Napoli mud volcano. B) Dendrogram obtained from clustering analysis of DGGE banding profiles and scoring bands as present or absent, using the R software. Bar indicates dissimilarity values.

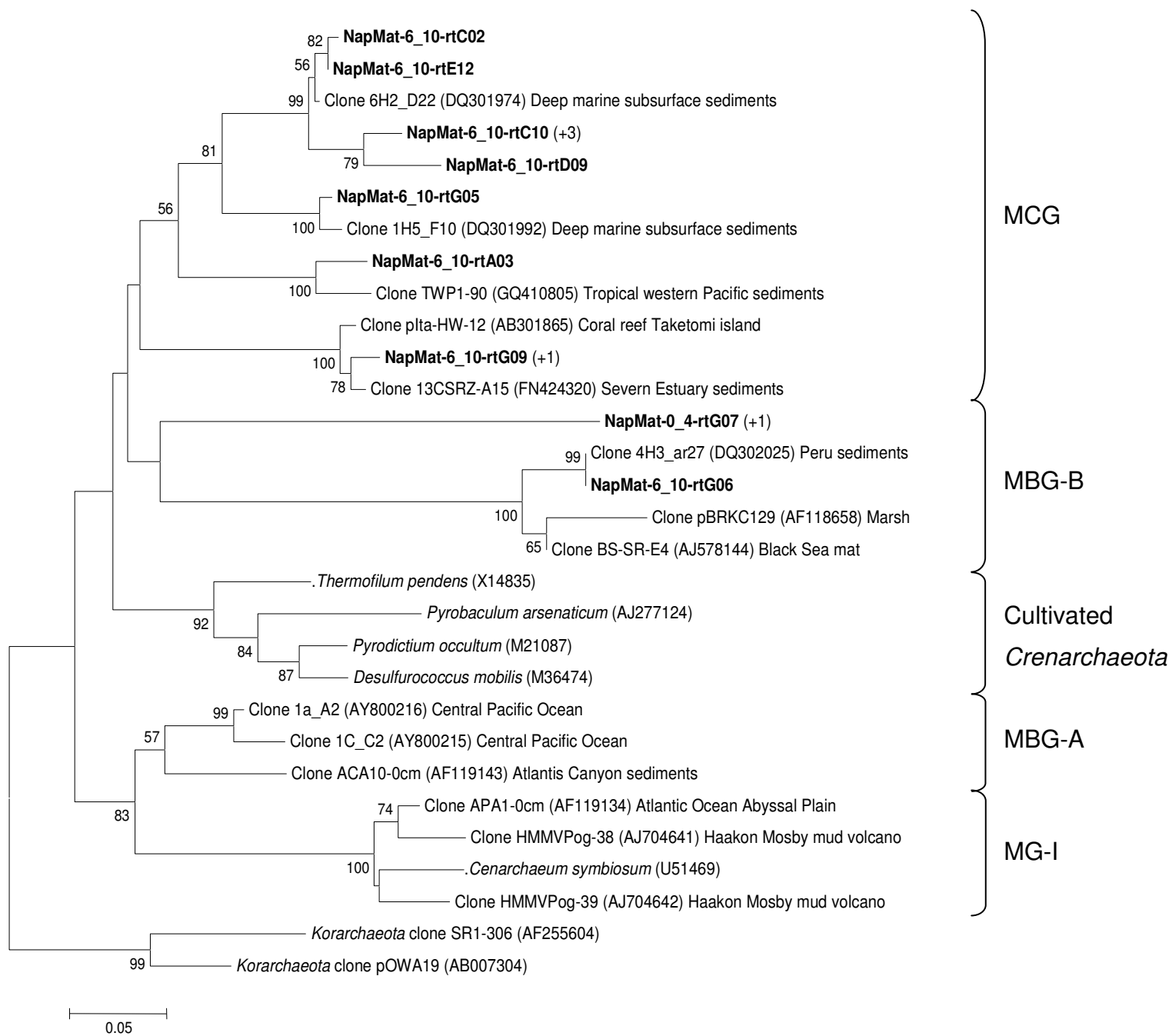
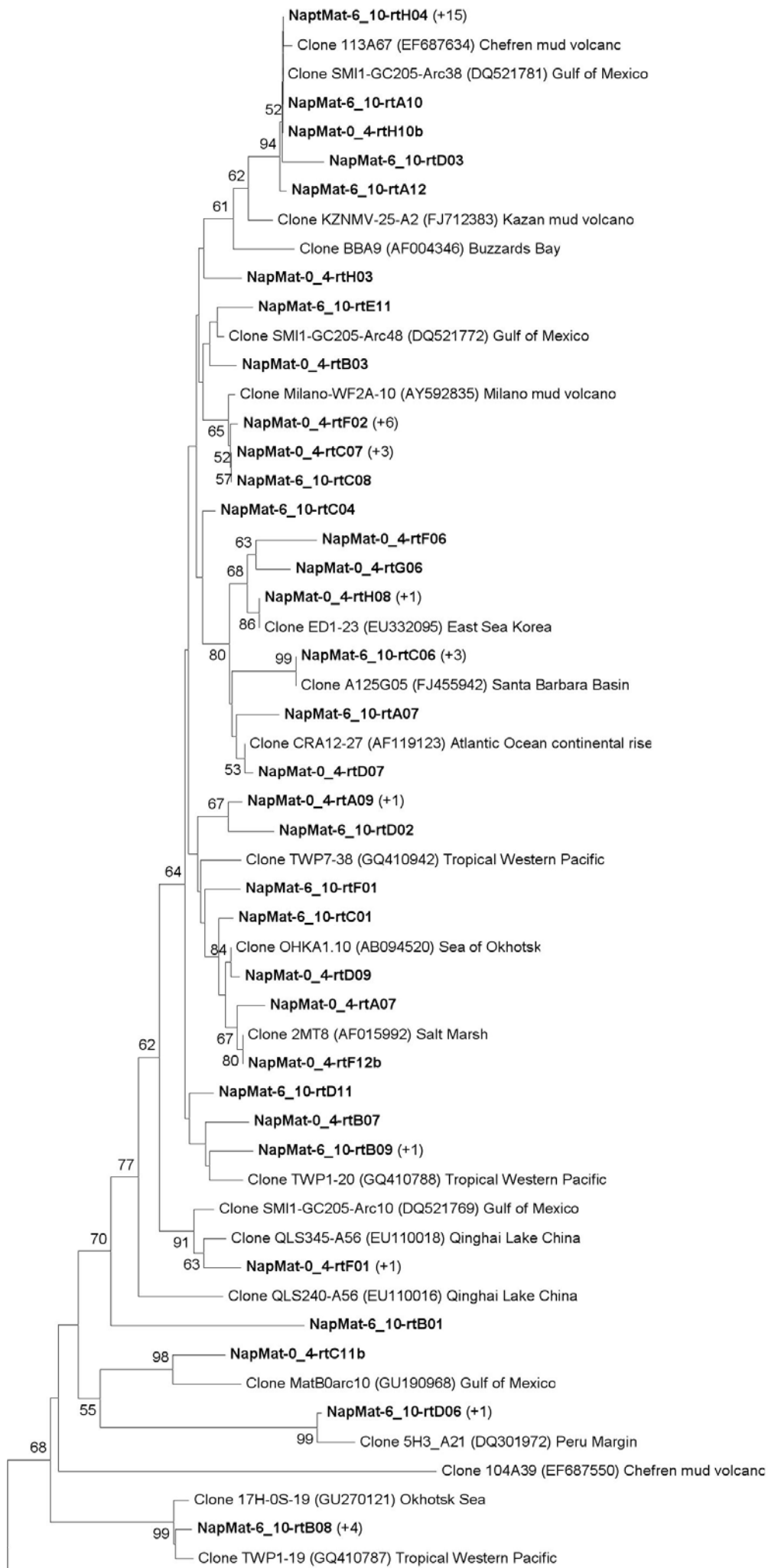


**Figure 4.** Phylogenetic analysis of the Crenarchaeal RNA-derived 16S rRNA genes of the Napoli mud volcano sediments based on the neighbour-joining method with 575 homologous positions. Bootstrap values (in percent) are based on 1000 replicates and are indicated at nodes for branches values  $\geq 50\%$  bootstrap support. Gene sequences recovered in this study from Napoli mud volcano sediments are in

boldface type. Clones with designation beginning NapMat-0\_4 and NapMat-6\_10 are from the sediment section 0 to 4 and 6 to 10 cmbsf respectively. Numbers in parentheses indicate the number of analyzed clones that have more than 97 % sequence identity. The scale bar indicates five substitutions per 100 nucleotides. MCG, Miscellaneous Crenarchaeotic Group, MBG-B, Marine Benthic Group B, MBG-A, Marine Benthic Group A, MG-I, Marine Group I.



MBG-D

TMEG

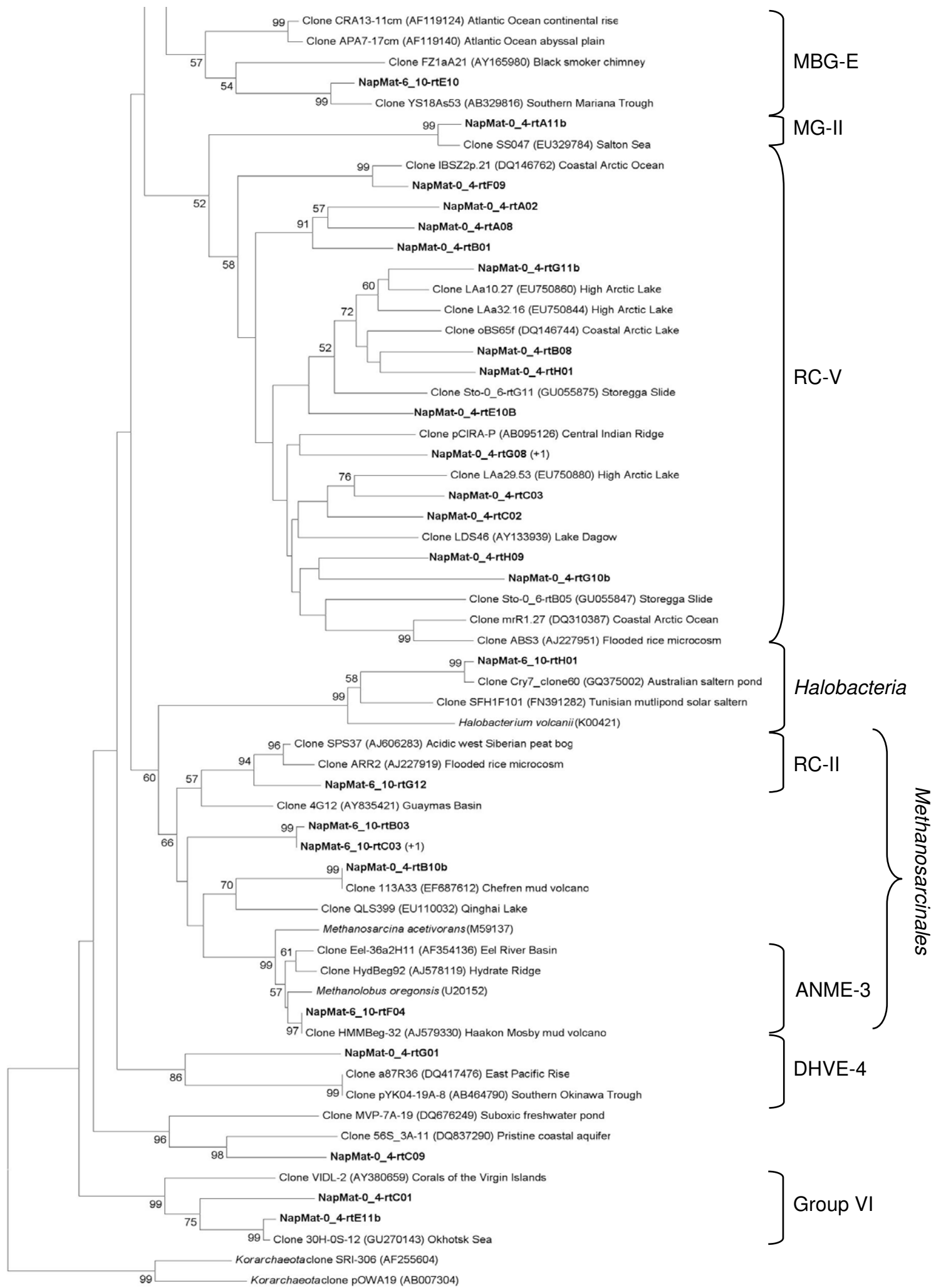
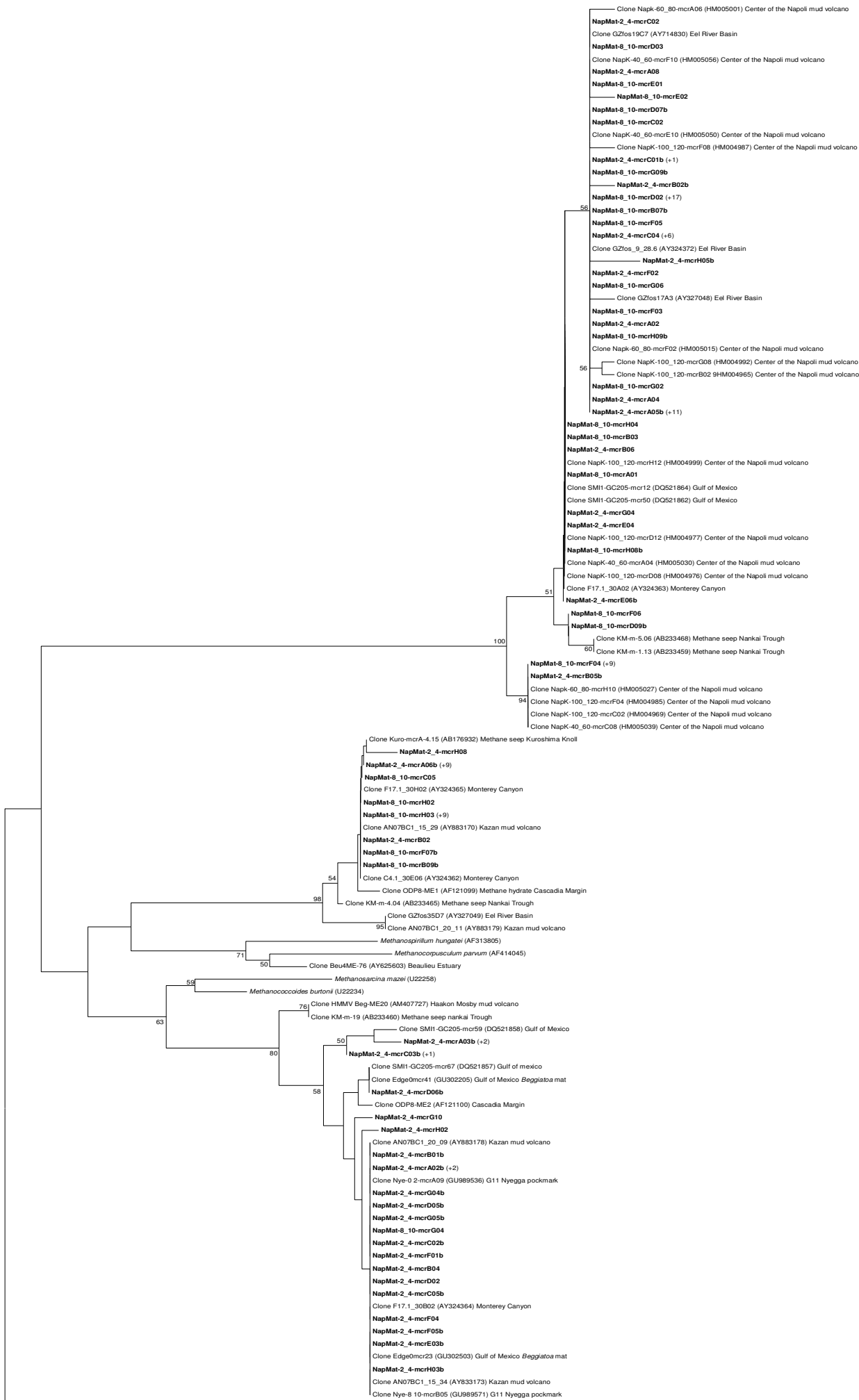


**Figure 5.** Phylogenetic analysis of the Euryarchaeal RNA-derived 16S rRNA genes of the Napoli mud volcano sediments based on the neighbour-joining method with 575 homologous positions. Bootstrap values (in percent) are based on 1000 replicates and are indicated at nodes for branches values  $\geq 50\%$  bootstrap support. Gene sequences recovered in this study from Napoli mud volcano sediments are in boldface type. Clones with designation beginning NapMat-0\_4 and NapMat-6\_10 are from the sediment section 0 to 4 and 6 to 10 cmbsf respectively. Numbers in parentheses indicate the number of analyzed clones that have more than 97 % sequence identity. The scale bar indicates two substitutions per 100 nucleotides. RC-V, Rice Cluster V, MBG-D, Marine Benthic Group D, TMEG, Terrestrial Miscellaneous Euryarchaeotal Group, MBG-E, Marine Benthic Group E, MG-II, Marine Group II, RC-II, Rice Cluster II, DHVE-4, Deep Sea Hydrothermal Vent Euryarchaeotal Group 4.





*mcrA* group a/b  
(ANME-1)

*mcrA* group c/d  
(ANME-2c)

*mcrA* group e  
(ANME-2a)

**Figure 6.** Phylogenetic analysis of MCR amino acid sequences from the Napoli mud volcano sediments based on the neighbour-joining method with approximately 258 amino acid positions. Bootstrap values (in percent) are based on 1000 replicates and are indicated at nodes for branches values  $\geq 50\%$  bootstrap support. Gene sequences from the Napoli mud volcano sediments obtained in this study are in boldface type. Clones with designation beginning NapMat-2\_4 are from the sediment section 2 to 4 cmbsf, and NapMat-8\_10 from sediment section 8 to 10 cmbsf. Numbers in parentheses indicate the number of analyzed clones that have more than 97 % nucleotide sequence identity, and more than 99 % amino acid sequence identity. The scale bar indicates 10 % estimated difference. ANME, Anaerobic Methanotroph.

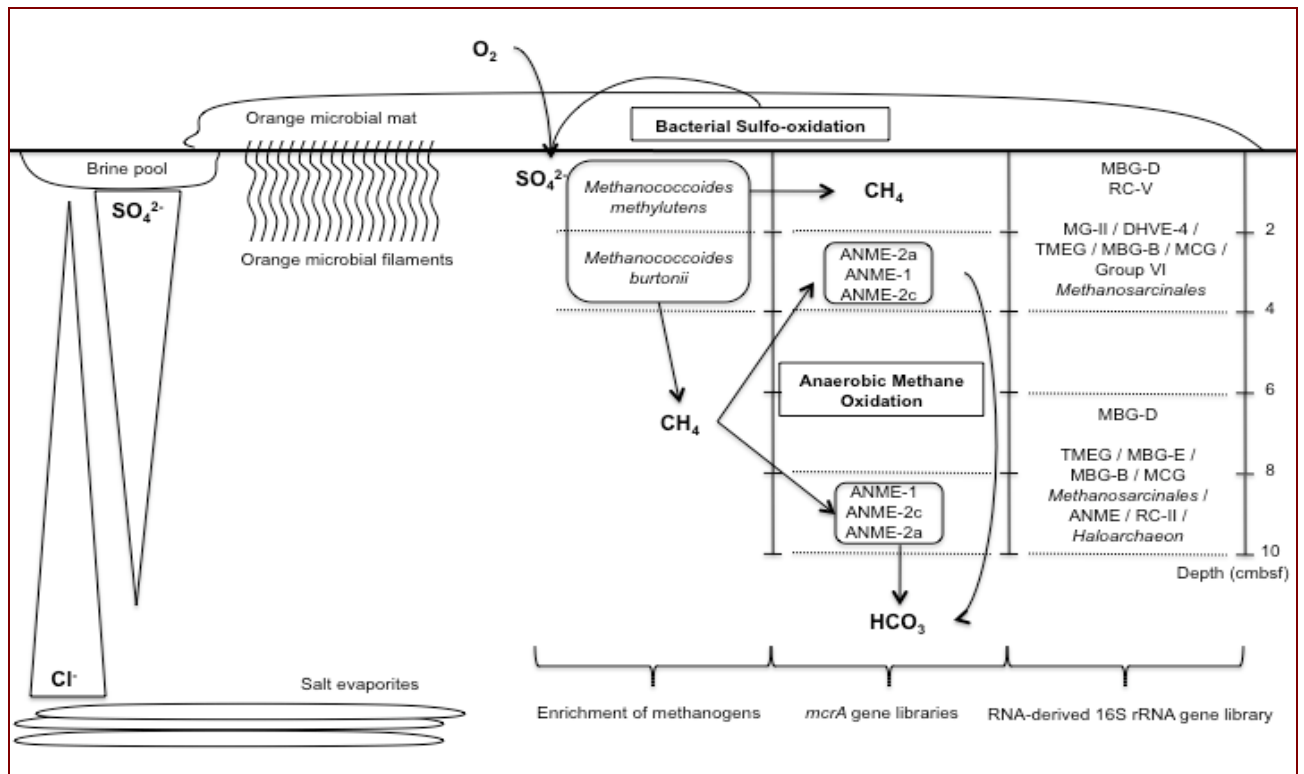


**Figure 7.** Schematic illustrating the potential interactions between anaerobic methanotrophic *Archaea* (ANME) probably mediating anaerobic oxidation of methane, methanogens, and uncultured *Archaea* in different hypersaline sediment sections of the Napoli mud volcano. Sediment depth below the seafloor is indicated at the right of the illustration.